Supplement of Geosci. Model Dev., 18, 2231–2248, 2025
https://doi.org/10.5194/gmd-18-2231-2025-supplement

Geoscientific Model Development
Open Access
EGU

Supplement of

Sensitivity studies of a four-dimensional local ensemble transform Kalman filter coupled with WRF-Chem version 3.9.1 for improving particulate matter simulation accuracy

Jianyu Lin et al.

Correspondence to: Tie Dai (daitie@mail.iap.ac.cn)

The formulation of RMSE, and correlation coefficient are shown below

$$RMSE = \sqrt{\frac{1}{N}\sum_{j=1}^{N}(M_j - O_j)^2} \quad \text{(S1)}$$

$$CORR = \frac{\sum_{j=1}^{N}(O_j - \bar{O})(M_j - \bar{M})}{\sqrt{\sum_{j=1}^{N}(O_j - \bar{O})^2 \sum_{j=1}^{N}(M_j - \bar{M})^2}} \quad \text{(S2)}$$

N is the total number of observations. J is the sample number of simulation and observation. M is the simulation results and the O is observation.

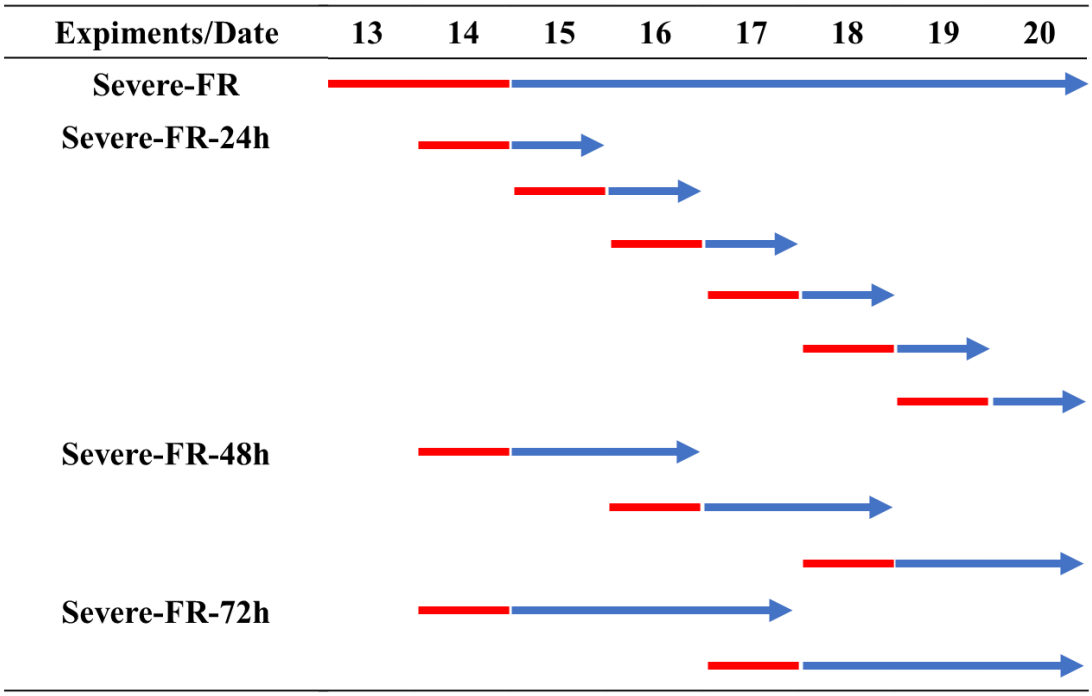

Figure S1. The spin up time (red bar) and integration time (blue arrows) of control experiments in this research.

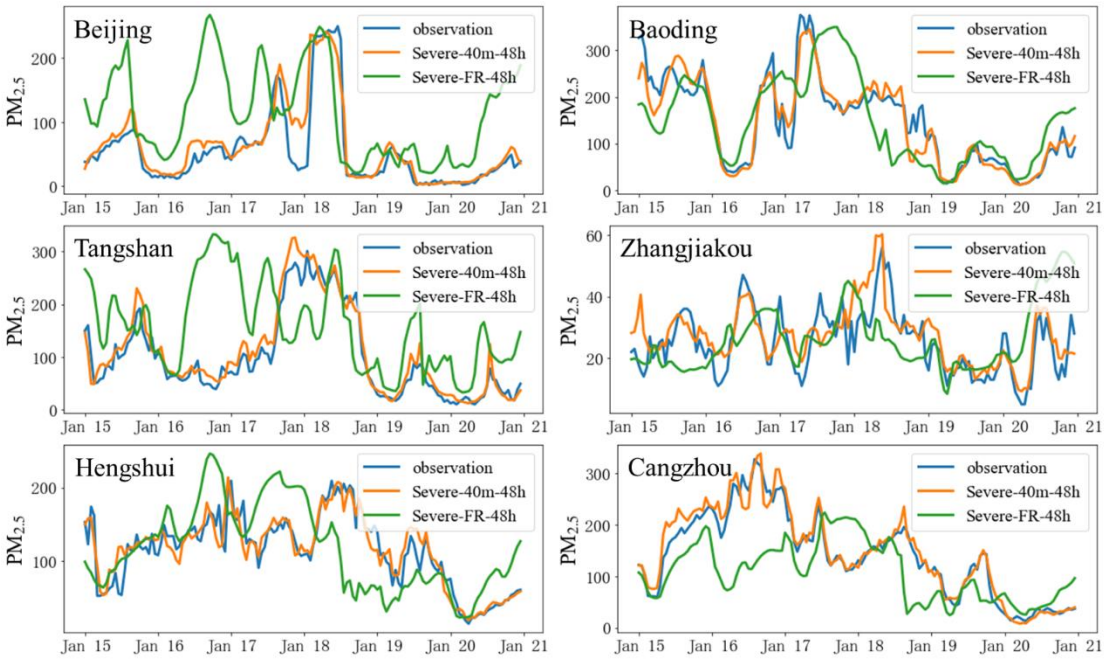

Figure S2. Temporal variations of $PM_{2.5}$ from Severe-40m-48h, Severe-FR-48h and observation at six independent verification stations (units: μg m^{-3}).

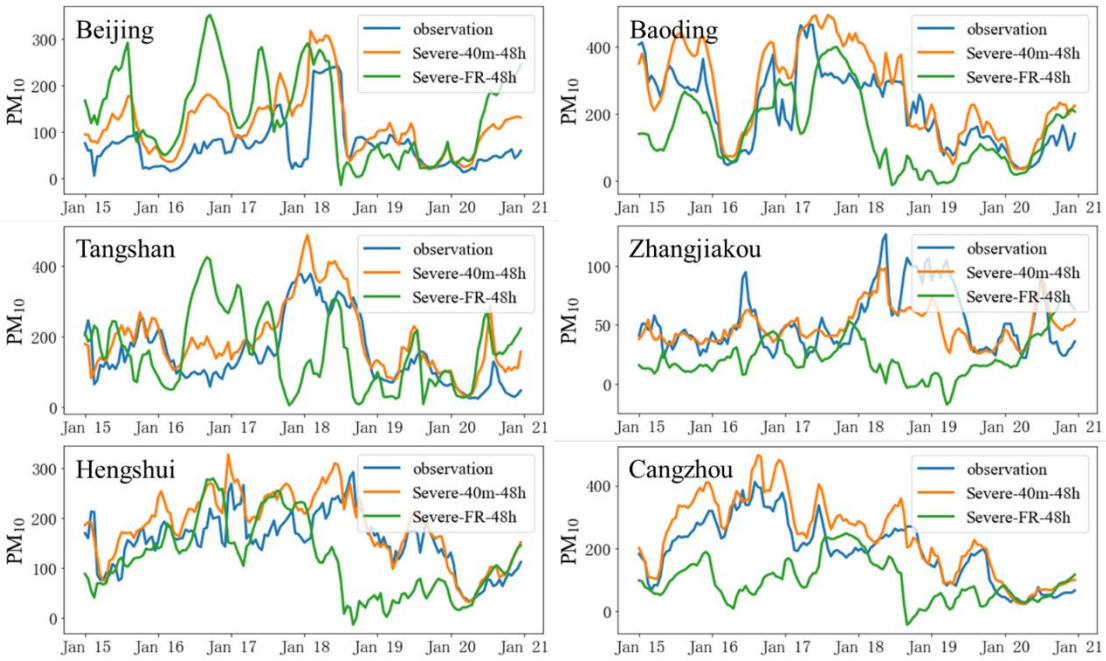

Figure S3. Similar with Figure S2 but for PM_{10}.

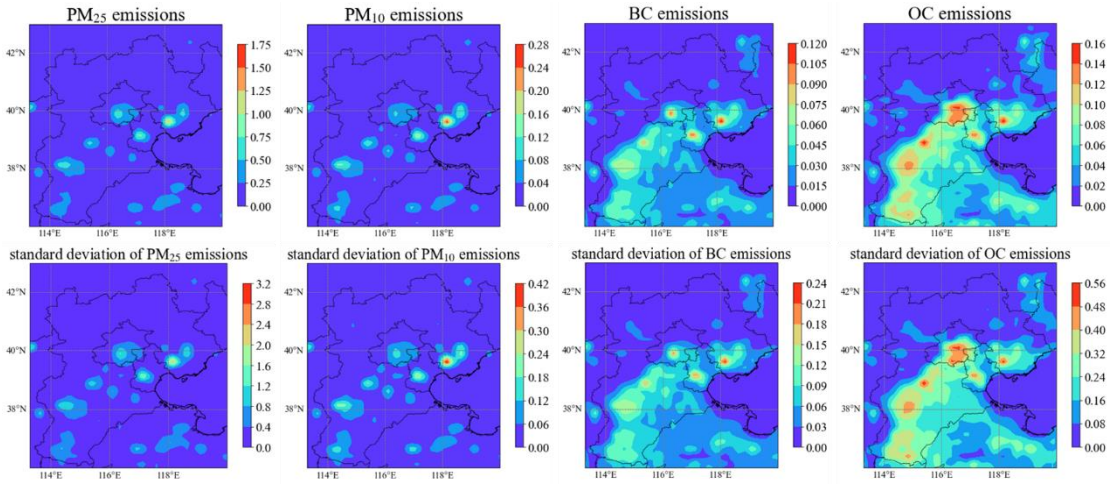

Figure S4. Contour maps about spatial distribution of anthropogenic $PM_{2.5}$, PM_{10}, BC and OC emissions in first row (units: $\mu g\ m^{-2}\ s^{-1}$) and their standard deviations calculated from 40 ensemble members in second row.

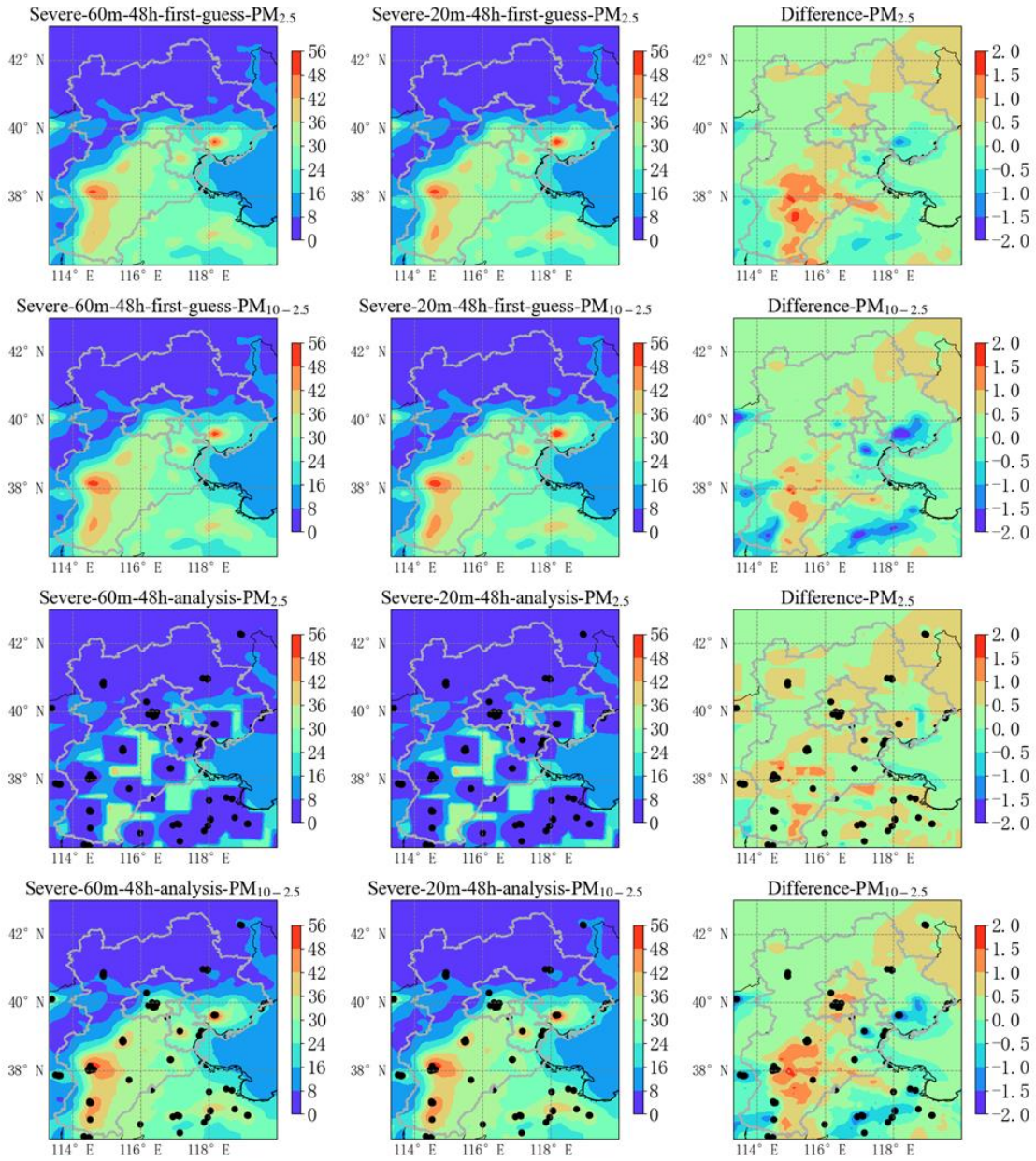

Figure S5. Contour maps of spatial distributions of temporal averaged $PM_{2.5}$ and $PM_{10\text{-}2.5}$ standard deviations in the first guess (first and second row) and analysis (third and fourth row) of (Severe-60m-48h minus Severe-20m-48h) within simulation period (units: μg m^{-3}). The black dots in analysis of $PM_{2.5}$ and $PM_{10\text{-}2.5}$ implies the location of assimilated stations. The grey border implies the BTH region.

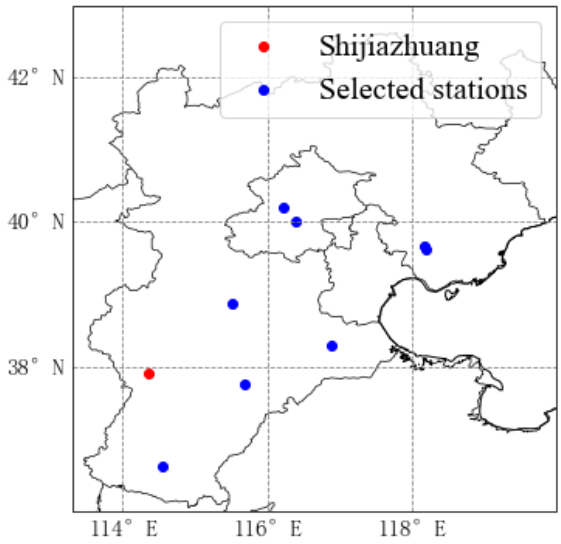

Figure S6. The geographical locations of observations of Shijiazhuang and selected stations.

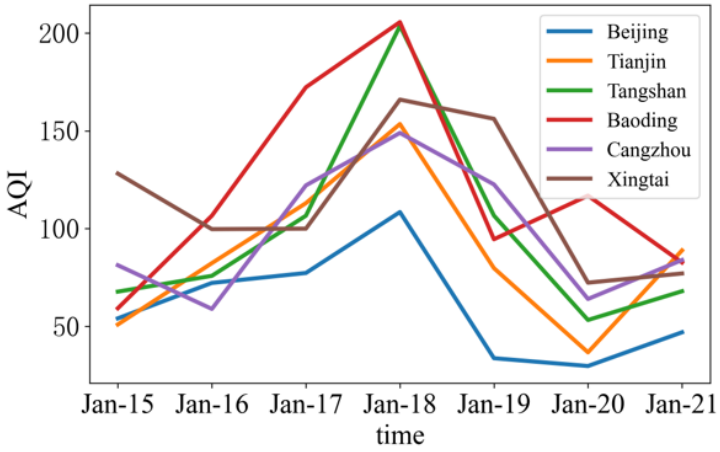

Figure S7. Temporal variation about air quality index at six representative sites in moderate haze event.

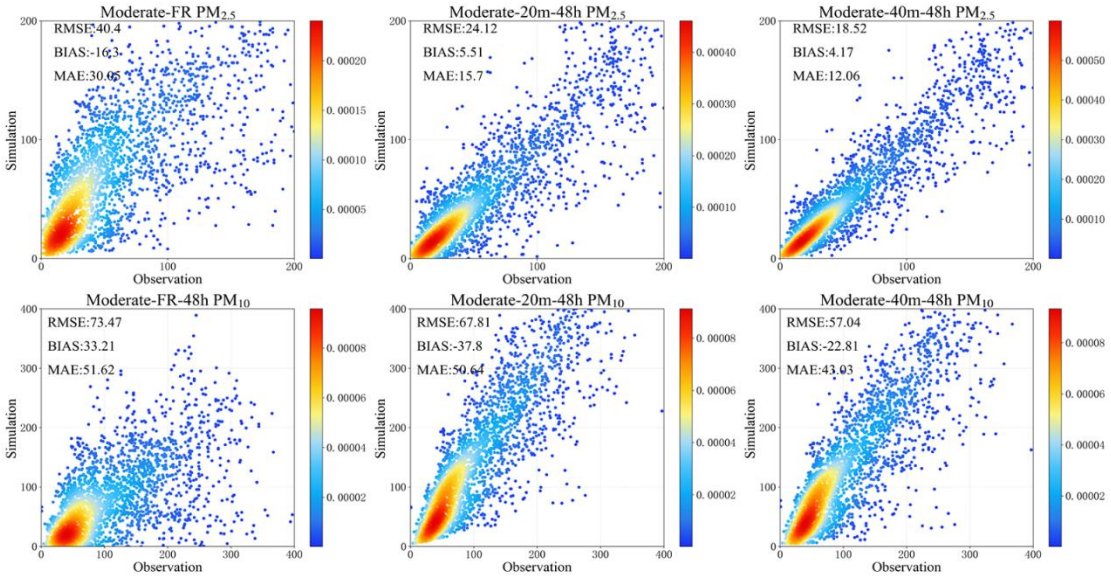

Figure S8. Scatter and density plots of $PM_{2.5}$ and PM_{10} observations from verification stations versus those in Moderate-FR-48h, Moderate-20m-48h and Moderate-40m-48h (units: $\mu g\ m^{-3}$).

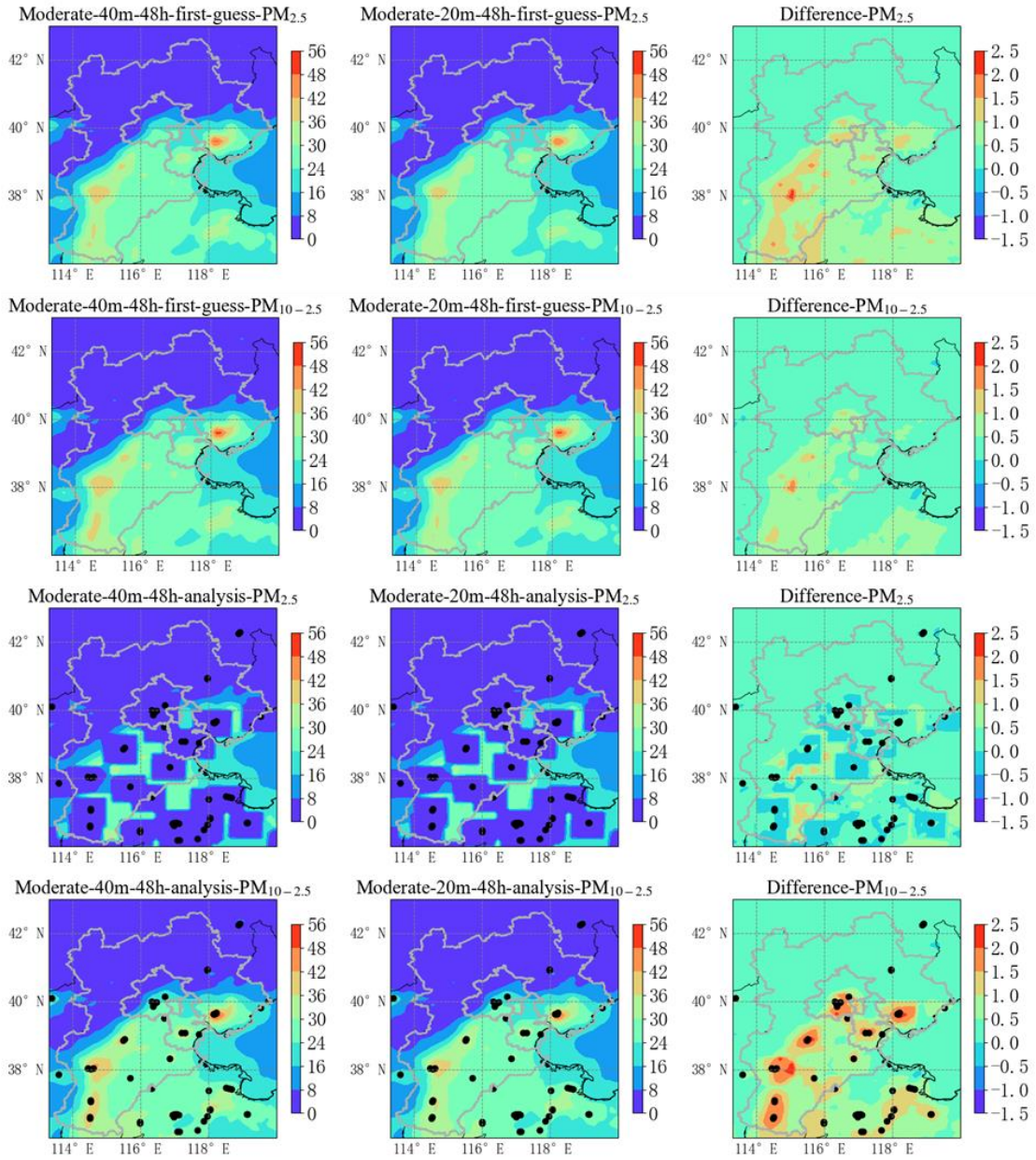

Figure S9. Contour maps of spatial distributions of temporal averaged $PM_{2.5}$ and $PM_{10\text{-}2.5}$ standard deviations in the first guess (first and second row) and analysis (third and fourth row) of Moderate-40m-48h, Moderate-20m-48h and their difference (Moderate-40m-48h minus Moderate-20m-48h) in a moderate haze event (units: μg m^{-3}). The black dots in analysis of $PM_{2.5}$ and $PM_{10\text{-}2.5}$ implies the location of assimilated stations. The grey border implies the BTH region.